Building and Environment 193 (2021) 107672

Contents lists available at ScienceDirect

Building and Environment

journal homepage: http://www.elsevier.com/locate/buildenv

Performance assessment of hygrothermal modelling for diagnostics and conservation in an Italian historical church

Francesca Frasca [a,*], Elena Verticchio [b], Cristina Cornaro [c], Anna Maria Siani [a]

[a] Department of Physics, Sapienza University of Rome, P.le Aldo Moro 5, Rome, Italy
[b] Department of Earth Sciences, Sapienza University of Rome, P.le Aldo Moro 5, Rome, Italy
[c] Department of Enterprise Engineering, University of Rome Tor Vergata, Via Del Politecnico 1, Rome, Italy

ARTICLE INFO

Keywords:
Historical churches
Hygrothermal modelling
Historical buildings
HAM model
Diagnostics
Conservation risks

ABSTRACT

The hygrothermal modelling of historical churches is a promising approach to study preservation issues and suitable retrofit measures. However, difficulties can arise in the use of Heat, Air and Moisture (HAM) models, which are often customised objects to be integrated into validated building energy simulation (BES). This research outlines a multi-step methodology to investigate the capability of a BES software coupled with a HAM model (BES + HAM) as a technique for diagnostics and conservation in complex settings. The 17th-century church of Santa Rosalia (Italy) was used as a historical site in a real context. As first step, the performance of the simulation tool was analysed through standardised exercises aiming at excluding incorrect assumptions and calculations in the HAM model (HMWall). Secondly, a building model of the church using a 1D heat transfer model (named building model A) was compared with one using HMWall (named building model B) in terms of the accuracy of the indoor climate simulations against hygrothermal measurements. The results showed that building model B enhanced the simulation accuracy by +50% with respect to building model A. Finally, annual simulations inside the church were run to further compare the seasonal trends of indoor climate scenario obtained from the two building models. Building model B allowed to study the water content distribution inside the altarpiece and a wall partition, showing that BES + HAM tools can be used to identify potential moisture-induced conservation risks.

1. Introduction

The number of historical churches is copious throughout Europe and especially in Italy, where churches, abbeys, cloisters, crypts and monastic complexes represent all together approximately the 30% of the total architectural monuments [1]. Historical churches often contain valuable interiors, which need to be adequately preserved; therefore, the development of suitable strategies for their preservation requires a thorough understanding of the climate-induced risks [2]. For example, hygroscopic furnishings and artworks conserved in churches can be severely damaged by relative humidity fluctuations. In addition, moisture condensation in poor ventilated or damp environments (e.g. crypts) may contribute to biological colonisation and crystallisation/dissolution of deliquescent salts [3]. As in the case of any other building, the indoor environment inside churches is influenced by the local climate and features of the building envelope as well as the management of the site (e.g. Ref. [4] for Mediterranean area and [5] for northern European regions). The conservation of churches can be also threatened by uncontrolled use of heating systems, because they adversely affect the indoor historic climate [6]. In the framework of the Friendly Heating project (2002–2005), the most suitable heating systems for churches were thoroughly studied [7]. Currently, the selection of heating strategies and the ventilation management for the protection of churches, chapels and other places of worship is regulated by the European standard EN 15759-1 [8].

In the last decades, the use of mathematical models has attracted a broad interest in the scientific community as a method to diagnose conservation conditions and to study the suitability of retrofit measures in historical buildings, including churches. An approach in indoor climate modelling is the use of transfer functions (TFs) that derive the indoor hygrothermal conditions from the outdoor climate [9]. A more powerful tool is the whole building dynamic simulation, which can provide both energy and hygrothermal assessment. In Climate for

* Corresponding author.
E-mail addresses: f.frasca@uniroma1.it (F. Frasca), elena.verticchio@uniroma1.it (E. Verticchio), cornaro@uniroma2.it (C. Cornaro), annamaria.siani@uniroma1.it (A.M. Siani).

https://doi.org/10.1016/j.buildenv.2021.107672
Received 28 September 2020; Received in revised form 16 January 2021; Accepted 1 February 2021
Available online 8 February 2021

Abbreviations

ΔRH	Daily RH rate (%·day^{-1})
τ_e	Solar light transmittance
τ_v	Visible light transmittance
ACH	Air Change per Hour
BES	Building Energy Simulation
CV-RMSE	Coefficient of Variation of the Root Mean Square Error
D_{ws}	Liquid transport coefficients for suction
D_{ww}	Liquid transport coefficients for redistribution
HAM	Heat Air and Moisture
MAE	Mean Absolute Error
MR	Mixing Ratio (g·kg^{-3})
p_{sat}	Saturated water vapour pressure
p_v	Water vapour partial pressure
Qv	Prediction rate
RMSE	Root Mean Square Error
RH	Relative Humidity (%)
rho	Correlation coefficient
SHGC	Solar Heat Gain Coefficient
T	Temperature (°C)
TF	Transfer function
TRY	Test Reference Year
U-value	Thermal transmittance
w	Water content (kg·m^{-3})

Hygrothermal properties of building materials in HMWall

λ	Thermal conductivity (W·m^{-1}·K^{-1})
ρ	Density (kg·m^{-3})
C	Specific heat (J·kg^{-1}·K^{-1})
w_f	Free water saturation (kg·m^{-3})
w_{80}	Equilibrium water content at RH = 80% (kg·m^{-3})
b	Thermal conductivity supplement (−)
μ	Vapour diffusion resistance (−)
A_w	Water absorption coefficient (kg·m^{-2}·s$^{-0.5}$)

Culture project (2009–2014) [10], the indoor climate conditions inside 35 churches located around Europe were simulated using various simulation software in order to investigate requirements for preventive conservation strategies (e.g. Refs. [11,12]). Coelho et al. [13] modelled a 13th-century church in WUFI Plus to study the accuracy of hygrothermal simulations in complex buildings such as churches. Sadłowska-Sałęga et al. [14] used indoor and outdoor climate data to validate a hygrothermal building model of a 18th-century wooden church in WUFI Plus, paying attention to the effect of input parameters in the accuracy of the results. Muñoz-González et al. [15,16] assessed passive, active and combined environmental conditioning techniques in two Spanish historical churches by means of Energy Plus. Two Estonian churches were modelled in IDA ICE to study the impact of adaptive ventilation strategies [17], dehumidification and heating systems on indoor climate and energy consumption [18]. Semprini et al. [19] evaluated the effect of HVAC system coupled with radiant devices for temperature and relative humidity control on the thermal comfort of visitors/churchgoers. Airing solutions in Sweden historical churches were evaluated by semi-empirical models [20] and IDA ICE [21] as an alternative to mechanical ventilation in removing contaminants threatening painted surfaces. Finally, the effect of future climate change on the preservation of artworks, thermal comfort and energy consumption was investigated in Ref. [22] by means of hygrothermal building models of three historical churches in parallel with on-site measurements.

A proper modelling of the indoor climate conditions is mandatory to take advantage from the simulation of the indoor climate, as it is directly and indirectly involved in all the deterioration processes of materials [23]. Consequently, whole building simulation tools need to accurately model the time behaviour of the key hygrothermal variables (e.g. temperature and relative humidity) responsible for degradation at short- and long-term scale, this being a necessary prerequisite in order to reliably use them for the design of advanced preventive conservation strategies. The main difficulty in the hygrothermal modelling of historical churches is the construction of the building model, which is demanding and time-consuming. In fact, each building has specific peculiarities due to the construction techniques and materials, resulting in a high risk of errors while modelling the building. In the hygrothermal modelling of historical buildings, Akkurt et al. [24] identified four sources of uncertainties: a) the geometrical model, b) the thermo-physical properties of the envelope, c) the schedules of internal gains and occupancy and d) the outdoor climate data. In this study, we focused on (b) source of uncertainty because the modelling of the simultaneous heat and moisture transfer through walls is essential in the dynamic simulation of historical buildings since most building materials are hygroscopic and can contain moisture at different thermodynamic phases. It follows that moisture and its related processes directly affect not only the thermal response of materials and their durability [25,26], but also the overall humidity inside a room (or zone) due to the sorption effect of hygroscopic materials [27].

Advanced and sophisticated models for indoor climate simulations are rarely employed in modelling historical buildings, as it can be difficult to dispose of robust algorithms and databases with the thermophysical and hygric properties of historical materials. Some building energy simulation tools (BES) integrate the heat and moisture flows through the algorithms of energy and mass balances between the air and hygroscopic surfaces [28,29] using HAM models, i.e. Heat, Air and Moisture models. The current approaches to model moisture exchanges in buildings are based on using either the co-simulation [30] or performing the hygrothermal calculations within the architecture of the building energy simulation (BES) software. In the co-simulation, each individual model is run in parallel (e.g. Refs. [31–33]) but two software are needed, i.e. the BES and the hygrothermal transfer model. Conversely, the second option has the main advantage of performing the hygrothermal assessment using a single simulation tool. IDA Indoor Climate and Energy (IDA ICE) extended with the HMWall model, having this advantage, was effectively exploited in several works including the modelling of historical buildings (e.g. Refs. [34,35]). To the best of our knowledge, not many studies have considered the moisture transfer modelling through walls, to cite a few: [11,12,14–16,22].

As all mathematical models are based on simplified parametrisations, the performance of the HAM models needs to be refined at different levels, from the building materials to the whole-building response [36]. This is particularly true when customised models are integrated into validated BES tool, as in the case of HMWall coupled with IDA ICE.

This study aimed to assess the performance of a BES software extended with a HAM model for diagnostics and conservation in historical churches through a multi-step methodology *ad-hoc* conceived. Since there is still no individual software or model nor an agreed method to perform the hygrothermal validation [37], standardised exercises were used to evaluate the performance of BES software coupled with HAM models. *Chiesa di Santa Rosalia* was chosen as a complex site to test the reliability of hygrothermal modelling for the preventive conservation of historical churches.

Sections 2.1 and 2.2 of this paper describe the site, the monitoring campaign and the construction of the building models. Section 2.3 explains the methodology developed to achieve the research objective. In section 3.1 and 3.2, the performance of HMWall (HAM model) into IDA

ICE (BES software) was assessed firstly in standardised exercises and then in the historical church of Santa Rosalia; section 3.3 dealt with the identification of some aspects of climate-induced conservation risks. Finally, section 4 is devoted to outline the main conclusions of the work and future research perspectives. A brief description of HMWall equations is given in Appendix A.

2. Materials and methods

2.1. Chiesa di Santa Rosalia: on-site climate measurements

The *Chiesa di Santa Rosalia* (Palestrina, Italy, Lat. 41.84° N and Long. 12.89° E, 550 m a.s.l.), hereafter simply called church, was chosen as a case study as its features well fit to the aim of this research. The north-east wall, corresponding to the chancel, is embedded in a rocky outcrop, from which liquid water can freely percolate from the soil to the walls. This could have caused the risk of superficial detachments and chromatic alterations of the cladding marble, leading the restorers to replace the original altarpiece with a copy.

The church was built in 17th-century enclosed into the heavy masonries of the prestigious palace of Barberini Family and is an aisleless church with a square-central plan covered by a groined vault. Walls are covered by polychrome marbles that adorn the two tombs of Cardinals Antonio and Taddeo Barberini (Fig. 1a). A reason of concern was the conservation of the *Pietà Barberini,* attributed to Michelangelo Buonarroti, that used to be preserved in the sacristy of the church and was moved to *Galleria dell'Accademia* in Florence (Italy) in 1938.

An indoor and outdoor climate monitoring was carried out to study the indoor hygrothermal behaviour of the church. Technical and financial reasons limited the monitoring period from January 1st till March 31st, 2015 and that period was chosen since climate conditions can favour the condensation on the walls. Two thermo-hygrometers (manufactured by Rotronic®, model HC2–S3) were placed inside the church to measure temperature (T) and relative humidity (RH): one T-RH probe (labelled as "TRH1" in Fig. 1a) was placed in a central position at 3 m height and the other in an empty space behind the altarpiece (labelled as "TRH2" in Fig. 1a). A third thermo-hygrometer of the same model, shielded from solar radiation by a small Stevenson screen, was placed on the terrace of the church to collect the outdoor T and RH conditions needed for the compilation of the climate file used in the simulation. T sensors were Pt100 resistance thermometers with an operating range −40°C-+60 °C and uncertainty of 0.3 °C; whereas RH sensors were thin film capacitive sensors with an operating range 0–100% and uncertainty of 1.5%. Both sensors were in accordance with the current European Standards about the metrological features of the instruments for measuring T and RH in cultural heritage conservation [38,39]. Moreover, a soil moisture sensor (labelled as "M1" in Fig. 1a) (manufactured by Meter Environment model ECH$_2$O EC-5) provided the measurements of the volumetric water content with an operating range between 0 and 1 $m^3 \cdot m^{-3}$ and an uncertainty of ±2% and was placed in a small crack located to a corner of the north-east wall.

All measurements were sampled every 5 min and recorded every 30 min as averaged values.

Indoor T and RH values do not show significant differences between

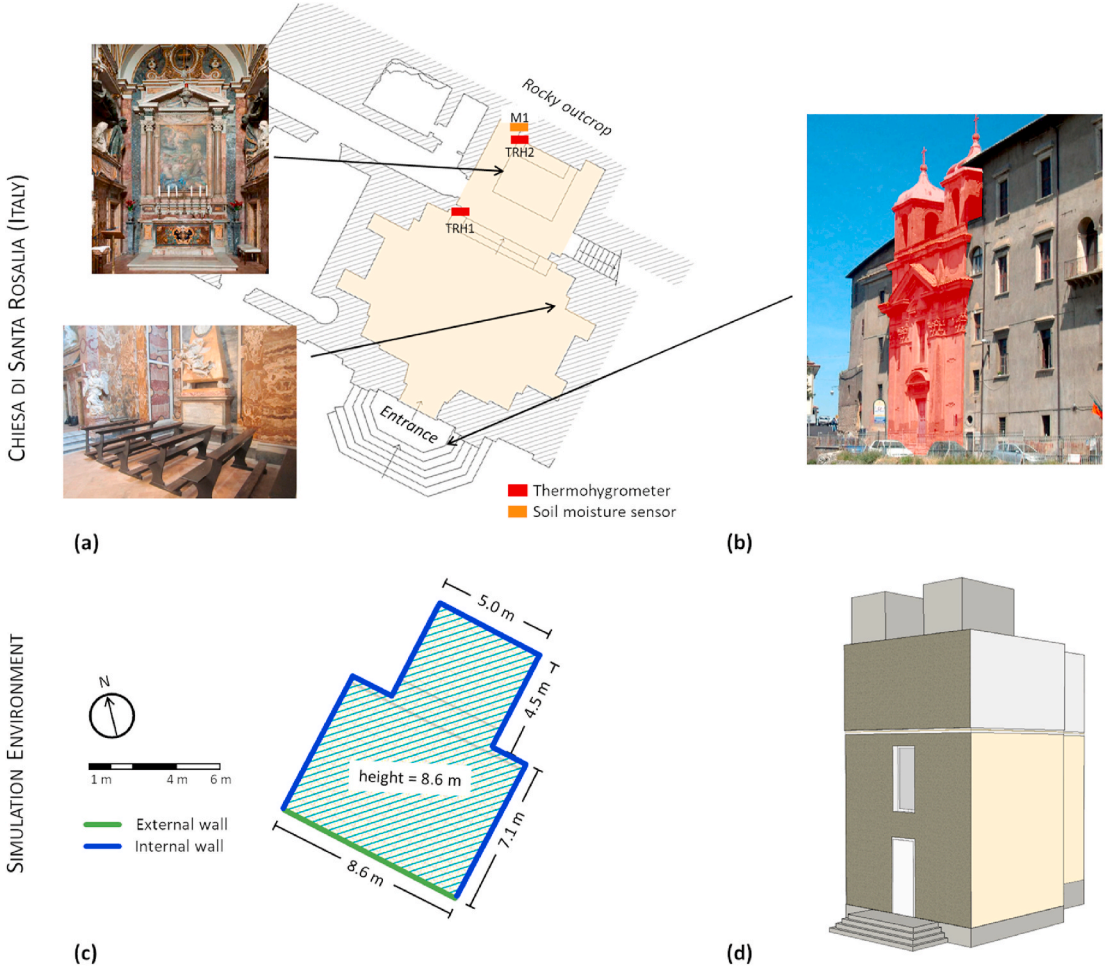

Fig. 1. (a–b) Plan of the Church of Santa Rosalia in Palestrina with the location of internal instruments together with internal [40] and external views; (c–d) floor plan and 3D model of the church in the IDA ICE environment.

the two sampling points. The minimum and maximum T values were 11.0–14.6 °C in "TRH1" and 10.5–18.7 °C in "TRH2", whereas for RH measurements they were 23.0–81.6% in "TRH1" and 21.0–79.5% in "TRH2". These outcomes show that the two areas were in hygrothermal equilibrium. The volumetric water content was constant at 0.114 $m^3 \cdot m^{-3}$ over the monitoring period and was considered as a marker of the moisture level.

2.2. Building model construction of the historical church

The building model of the church was created encompassing (i) indoor and outdoor climate measurements and (ii) architectural surveys carried out by the authors. The former (i) was used to calibrate building model, the latter (ii) to reduce the main uncertainties in the building model as reported in Ref. [24]. The 3D model of the church sketched in IDA ICE is shown in Fig. 1d. The building model consisted of five zones reproducing the church (Fig. 1a,c-d) and the adjoining spaces (not shown in Fig. 1c and d), which were included to estimate both the horizontal and the upward heat transmittance. The total floor area and the total volume of the church were 75.3 m^2 and 608.1 m^3, respectively.

The main difficulties encountered during the construction of a reliable building model regarded the modelling of the rocky outcrop and the simplification of internal geometries as well as walls' orthogonality to keep unchanged the total internal volume (Fig. 1c). The rocky outcrop behind the north-east wall was modelled as ground based on EN ISO 13370:2017 [41] and connected to the wall. This wall was divided in two partitions, the heavy masonry and the wooden altarpiece, due to their considerable thickness (1.06 and 0.05 m, respectively).

First, a thermal building model (hereafter named building model A) was created in IDA ICE environment modelling the walls through a 1D heat transfer model. Then, this wall model was replaced with HMWall (hereafter named building model B) in order to assess whether the building model B may outperform the building model A.

As shown in Fig. 1c, there are six internal walls considered adiabatic due to their considerable thickness, one internal wall adjoining the rocky outcrop and one external wall. When the 1D heat transfer model was replaced with HMWall, moisture connections were added. The moisture connections are identified as RH connections since both moisture flows are driven by the RH gradient. The internal side of walls was connected to the indoor T and RH of the zone. The external side of the external wall was connected to the T and RH values of the climate file. The back side of walls was set to a constant RH values of 50% except for the north-east wall, set to a constant 95% RH, based on the measurements of the water content ("M1"). As for the altarpiece, the back side was set to 80% RH as a compromise between measurements ("TRH2"). The initial conditions of moisture content (w) inside walls were homogeneously set to w values corresponding to RH = 50% in internal/external walls and to a RH gradient from 50% (internal side) to 100% (back side) in the north-east wall to consider the effect of the water infiltrations from the rocky outcrop. The stratigraphy of walls was

Table 1
Hygrothermal and physical properties of the horizontal and vertical opaque components per each partition according to the values obtained after the calibration of the building model with the climate measurements (from internal side to external side).

Input parameters										
Partition	Material (thickness in m)	Total thickness	Thermal conductivity	Density	Specific heat	Equilibrium water content at RH = 80%	Free water saturation	Thermal conductivity supplement	Vapour diffusion resistance	Water absorption coefficient
		s m	λ $W \cdot m^{-1} \cdot K^{-1}$	ρ $kg \cdot m^{-3}$	c $J \cdot kg^{-1} \cdot K^{-1}$	w_{80} $kg \cdot m^{-3}$	w_f $kg \cdot m^{-3}$	b –	μ –	A_w $kg \cdot m^{-2} \cdot s^{-0.5}$
External Wall	marble (0.02)	2.11	3	2300	880	0.9	69	4	530	0.003
	calcareous mortar (0.02)		0.8	1900	850	45	210	4	19	0.03
	tuff (2.0)		0.48	1450	925	75.7	259	4	10.4	0.10
	calcareous mortar (0.02)		0.8	1900	850	45	210	4	19	0.03
	plaster (0.05)		0.7	1600	850	30	250	4	7	0.05
Internal Wall	marble (0.02)	1.06	3	2300	880	0.9	69	4	530	0.003
	calcareous mortar (0.02)		0.8	1900	850	45	210	4	19	0.03
	tuff (1.0)		0.48	1450	925	75.7	259	4	10.4	0.10
	calcareous mortar (0.02)		0.8	1900	850	45	210	4	19	0.03
Altarpiece	gesso (0.01)	0.05	0.3	850	1000	6.3	400	4	8.3	0.29
	wood (0.04)		0.3	685	1500	115	500	4	8	0.01
Floor	cotta brick (0.06)	0.42	0.96	1952	863	123	161	4	19.4	0.14
	calcareous mortar (0.06)		0.8	1900	850	45	210	4	19	0.03
	tuff (0.3)		0.48	1450	925	75.7	259	4	10.4	0.10
Roof	roof brick (0.3)	0.30	1	1800	840	–	–	–	–	–
	calcareous mortar (0.05)		0.9	1800	910	–	–	–	–	–
	tiles (0.05)		1.16	2300	840	–	–	–	–	–

defined during the on-site survey of the church. As the hygrothermal and physical properties of walls could not be measured, those properties were gathered from the *MASEA Datenbank* [42] by choosing the most fitting materials and then adjusting the values of the parameters through the calibration procedure (described in Section 2.3.2). The values of the hygrothermal and physical properties of the opaque components are reported in Table 1.

The only window (1.5 × 3.0 m with a recess depth of 0.3 m) located on the south-west façade was made of a single pane glazing and a steel frame (20% of the total window area) with a thermal transmittance (U-value) of 5.8 and 2.0 $W \cdot m^{-2} \cdot K^{-1}$, respectively. As a layer of fine particles of dust were deposited on the vertical panes of the window, a shading component was added considering 40% of transparency [43]. The Solar Heat Gain Coefficient (SHGC), solar light transmittance (τ_e) and visible light transmittance (τ_v) of the single pane were set at 0.63, 0.50 and 0.45, respectively. In addition, internal thermal masses were added to take into consideration the heat transmittance of wooden furniture (e.g. pews) and other sculptures. Infiltrations were fixed at 0.05 ACH (Air Changes per Hour) mainly due to the door and the window at the façade, whereas thermal bridges were set at 0.04 $W \cdot m^{-1}$ per perimeter of both window and entrance door. Finally, hygrothermal gains and occupancy were set to zero as the number of churchgoers/-visitors was very limited and no hygrothermal sources were present in the church during the climate monitoring.

The climate file was created using hourly T and RH data measured by thermo-hygrometer placed on the terrace of the church. Local measurements are the most representative in whole building dynamic simulation in case of the Test Reference Year (TRY) files that are not suitable for climate model calibration [13]. Hourly wind (intensity and direction) and solar radiation (direct and diffuse) observations collected at *ESTER weather station – University of Rome Tor Vergata* (Lat. 41.86° N and Long. 12.62° E) were included into the climate file, as they were not measured *in situ*. The relatively short distance between the two sites (~21 km) led to similar levels of solar irradiances, especially in winter where weather patterns are mainly controlled by the large-scale air motions.

2.3. Methodology

A multi-step methodology was structured as shown in the schematic workflow of Fig. 2: (a) performance assessment of BES + HAM in standardised exercises (section 2.3.1); (b) performance assessment of BES + HAM in complex settings (section 2.3.2); (c) diagnostics and conservation scenario (section 2.3.3). Step (a) was conceived to pinpoint incorrect assumptions and calculations of HMWall into IDA ICE. Step (c) focused on evaluating the influence of outdoor climate on indoor conditions as well as the climate-induced conservation risks. Depending on results from steps (a) and (b), step (c) can be carried out.

2.3.1. Performance assessment of BES + HAM in standardised exercises

A multi-stage evaluation was conceived to explore the HAM (HMWall) capability in BES (IDA ICE) to model the hygrothermal distribution at wall-level and the influence of wall hygrothermal buffering at zone-level. Three exercises were *ad hoc* designed to understand whether the simulation tool might be able to also address conservation-related issues. Table 2 summarises the main features of the exercises reporting how HMWall is used in IDA ICE, the type of evaluation according to criteria defined in ANSI ASHRAE Standard 140 [47], the investigated process mechanism and the conservation-related issues.

2.3.1.1. Semi-infinite wall (exercise 1). This exercise was chosen to analyse the capability of HMWall to model the hygrothermal distribution inside a wall to estimate more accurately the risk of interstitial condensation. This feature is crucial in the hygrothermal modelling of historical buildings, as it allows to prevent deterioration of walls, such as mechanical damage due to mould infestation, thawing/freeze cycles or crystallisation/dissolution cycles of deliquescent salts, etc.

This exercise is based on the minimisation of hygrothermal curves reported in the European Standard EN 15026:2007 [44], where a detailed description of the exercise is given in Annex A. The modelled distributions of temperature (T) and moisture content (w) inside the material were compared with the range of the T and w values in the Standard. The hygrothermal properties used to run models are listed in Table 3 (first row).

2.3.1.2. Adiabatic building envelope (exercise 2). This exercise was formulated to study the performance of HMWall to estimate the extent of the moisture transfer by itself in the balance of RH inside a room (zone). This feature is useful in the case of historical buildings when there are inaccessible rooms/parts being completely airtight.

The description of this exercise is reported in detail in Ref. [45]. The simulations were performed over 8760 h at 1-h step (i.e. one whole year)

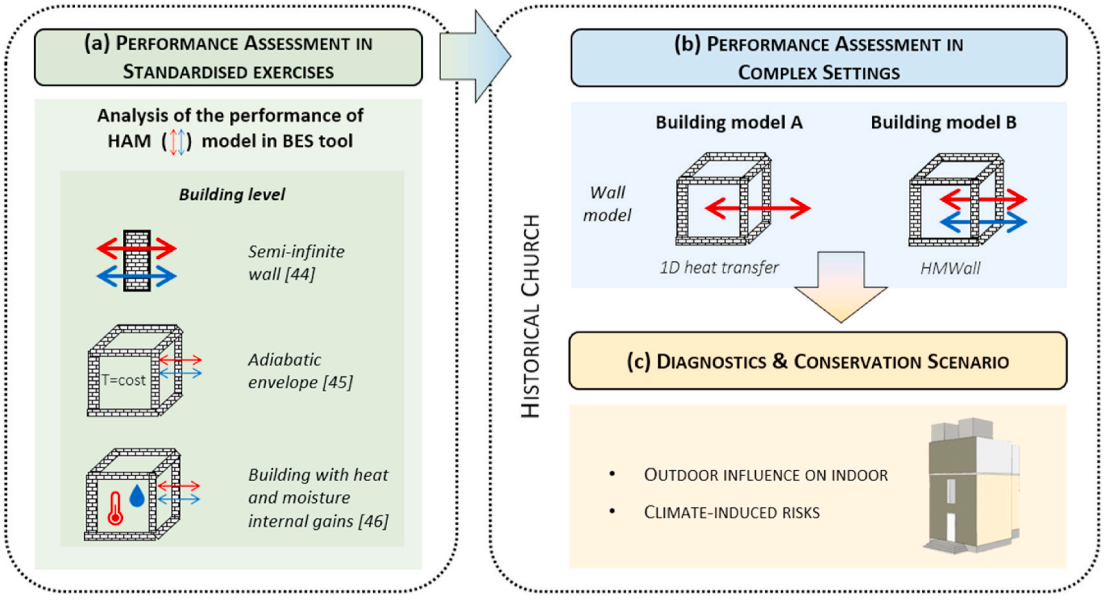

Fig. 2. Workflow of the performance assessment of the hygrothermal modelling (a–b) and diagnostics (c) in historical churches.

Table 2
Summary of the multi-stage evaluation of the BES + HAM performance.

Exercise	Ref	HMWall	Evaluation	Process mechanism	Conservation-related issues
1. semi-infinite wall	[44]	independent wall-object	analytical verification	superficial and/or interstitial condensation	mechanical damage due to thawing/freeze cycles or to crystallisation/dissolution cycles of deliquescent salts, mould infestation
2. adiabatic building envelope	[45]	wall-object of larger system	comparative test	indoor relative humidity solely due to the moisture transfer through walls	hygrothermal conditions in inaccessible rooms/parts completely airtight
3. building envelope with heat and moisture internal gains	[46]		empirical validation	indoor relative humidity affected by the moisture sorption effect of building materials	restoration interventions and retrofit measures

Table 3
List of hygrothermal properties used in HMWall for exercise 1 and used both in HMWall and in WUFI Plus for exercise 2.

Exercise	Input parameters							
	Thermal conductivity	Density	Specific heat	Free water saturation	Equilibrium water content at RH = 80%	Thermal conductivity supplement	Vapour diffusion resistance	Water absorption coefficient
	λ $W \cdot m^{-1} \cdot K^{-1}$	ρ $kg \cdot m^{-3}$	c $J \cdot kg^{-1} \cdot K^{-1}$	w_f $kg \cdot m^{-3}$	w_{80} $kg \cdot m^{-3}$	b –	μ –	A_w $kg \cdot m^{-2} \cdot s^{-0.5}$
1. Semi-infinite wall	1.5	1000.0	1842.0	146.0	87.6	10.5	227.8*	0.10×10^{-2} (*)
2. Adiabatic building envelope	1.0	1830.0	850.0	257.1	27.5	4.0	27.0	0.59×10^{-2}

* Average values referred to those provided by the Standard in the RH range 50–95%.

in an adiabatic building envelope completely airtight. The hygrothermal properties of the walls made of a 0.2 m monolayer of lime silica brick used to run models are listed in Table 3 (second row). It is worth noticing that, in this exercise, the variations of indoor relative humidity (RH_{in}) from initial condition at 50% depend only on the water vapour partial pressure (p_v) gained by the walls, because the saturated pressure (p_{sat}) is set to be constant ($T_{in} = T_{out} = 10$ °C). Three sorption processes driven by the RH indoor-outdoor gradient were considered: 1) moisture adsorption ($RH_{out} = 60\%$); 2) moisture desorption ($RH_{out} = 40\%$); 3) moisture seasonal trends (RH_{out} ranging periodically between 40% and 60%). The evaluation was based on a comparative test with the simulations run by WUFI Plus software, which is one of the most robust and validated hygrothermal simulation tools (e.g. Refs. [48–50]).

2.3.1.3. Two parallel rooms with internal moisture and heat gains (exercise 3). This exercise was chosen to study the performance of HMWall in modelling the moisture sorption effect of hygroscopic materials and hence their influence in the indoor RH values. The capability of a hygrothermal model to accurately reproduce the moisture sorption effect is pivotal in the simulation of historical buildings, as it regulates the short-term fluctuations of RH neither related to the day/night cycle (i.e. temperature) nor external factors (moisture ex/infiltration). This feature is essential for an advanced preventive conservation technique because it can guide restorers to the choice of restoration interventions and retrofit measures in accordance with conservation requirements.

The Common Exercise 3, developed in the framework of the Annex 41 of the International Energy Agency (IEA) Energy Conservation in Buildings and Community Systems program (ECBCS) [46], was used in this exercise as benchmark. It was applied for validating TRNSYS–COMSOL co-simulation tool [33] and for validating WUFI Plus and HAMBase simulation tools in the European project *Climate for Culture* (2010–2014) [51]. The experiments consisted of three tests in two rooms at constant T = 20.0 °C: reference room and test room. While the cladding materials of the reference room were kept unchanged during the tests, those of the test room's walls was changed as follows: Test1- aluminium foils on the walls (from January 17th till February 2nd); Test2- gypsum boards on the walls (from February 14th till March 20th); and Test3- gypsum boards on the walls and roof (from March 27th till April 16th). The indoor RH simulations were compared with RH measurements collected in the three experiments set up for the exercise (data provided by Florian Antretter and Kristin Lengsfeld, 2017).

2.3.2. Performance assessment of BES + HAM in the historical church

The performance of the BES + HAM in complex sites was assessed based on the comparison of the simulations against measurements in the historical church under study.

The building model A (BES + 1D heat transfer model) was calibrated using the indoor T and RH measurements at "TRH1" (Fig. 1a). The calibration was carried out from January 1st till January 31st, 2015 (1488 records), applying an automatic procedure in two steps for fine-tuning the values of: thermo-physical properties of partitions (initial values ± 10%), air infiltration (from 0.05 to 1ACH) and thermal bridges per perimeter of window and entrance door (from 0.00 to 0.10 $W \cdot m^{-2} \cdot K^{-1}$). As first step, a sensitivity analysis based on the Elementary Effect method was carried out identifying air infiltration for both T and RH as the most influencing input. Then, a genetic algorithm was used to minimize the Root Mean Square Error (RMSE) between modelled and measured T-RH data. The fine-tuned input parameters are reported in Section 2.2. The initialisation was set from November till December to take into account the effect of thermal inertia and moisture transfer in old thick masonries.

The validation of the building model was performed from March 1st till March 31st, 2015 (1488 records) with initialisation from January till February. Once building model A was calibrated, HMWall replaced the 1D heat transfer model in building model B so to assess whether it outperformed building model A.

Four statistical metrics were used to assess the accuracy of the hygrothermal simulations: the Mean Absolute Error (MAE), the Root Mean Square Error (RMSE), the Coefficient of Variation of RMSE (CV-RMSE) and the Spearman's correlation coefficient (rho) [52]. The assessment of the accuracy of the building models was extended to mixing ratio (MR, calculated from T and RH values [39]) as moisture mass-related variable. In addition, QQ-plots (quantile-quantile plot) were used to evaluate the agreement between modelled and measured

T-RH [12] and MR values as follows: high agreement, if data are within ±5% for RH and ±1°C for T and ±0.5 g·kg^{-1} for MR, good agreement, if data are within ±10% for RH and ±3°C for T and ±1.5 g·kg^{-1} for MR and poor agreement, if data are beyond ± 10% for RH and ±3°C for T and ±1.5 g·kg^{-1} for MR. Other criteria used to accept the building models as calibrated are CV-RMSE less than 30% [53] and rho higher than 0.8. Furthermore, the prediction rate (Qv) was used to evaluate the accuracy of the simulation in reproducing the daily fluctuations of RH [12].

2.3.3. Diagnostics and conservation in the historical church

It has to bear in mind that the hygrothermal modelling for diagnostics and conservation of historical churches can be pursued only if a reliable hygrothermal software is available and the building model is correctly calibrated with indoor climate measurements. If the performance assessment of the hygrothermal tool fits the requirements of the standardised exercises (section 2.3.1), then we can assume that the simulation of a building model calibrated over a calendar year or at least in different seasons (section 2.3.2) can be transferred to other periods where indoor climate measurements are not available. In this way, the indoor climate scenario from simulations can disclose potentially risky conditions for conservation.

This assumption allowed to further compare the performance of the hygrothermal modelling using 1D heat transfer with respect to HAM transfer through walls. Although calibration and validation were carried out in one season only, the results of the annual simulations can be meaningful for the comparison of the hygrothermal modelling with and without the HAM transfer, even if not fully representative of the actual indoor climate inside the church.

Indoor monthly averages of T and mixing ratio (MR) were plotted against outdoor ones to evaluate the seasonal behaviour of heat and moisture exchanges driven by external conditions.

In addition, building model B (BES + HAM) allowed to assess the moisture content distribution inside the moisture-sensitive partitions. Thus, moisture content distributions inside the north-east wall and the altarpiece were studied to ascertain whether they could threaten the conservation of moisture-sensitive and multi-layered objects.

3. Results and discussion

The preliminary performance evaluation of the heat and moisture transfer model used in this research is presented and discussed in section 3.1. Then, the results obtained using building model A and building model B of the church are analysed in section 3.2.

3.1. Performance assessment of BES + HAM in standardised exercises

3.1.1. Semi-infinite wall (exercise 1)

The hygrothermal profiles of the semi-infinite wall modelled by HMWall (blue dots) and the range of validity limits given in Ref. [44] (red area) are shown in Fig. 3. Both T (Fig. 3a–c) and w (Fig. 3d–f) distributions were satisfactorily reproduced by simulations with HMWall, although after 365 days w tended to diverge from the lower limit of the validity band. Indeed, the profiles were always within the validity limits along the whole wall thickness.

A limitation of HMWall is that discrete function values of hygrothermal curves cannot added. This feature can be pivotal when experimental data are available and when the hygrothermal curves of the materials cannot be adequately described by the HMWall functions.

3.1.2. Adiabatic building envelope (exercise 2)

Fig. 4 shows the scatter diagrams of modelled RH values (HMWall *versus* WUFI Plus) over a whole year for the three sorption processes considered (from Case 1 to Case 3). A strong agreement was found between RH values modelled by the two software. However, when RH_{out} = 40% (Fig. 4b), IDA ICE tended to reach the equilibrium with the outdoor

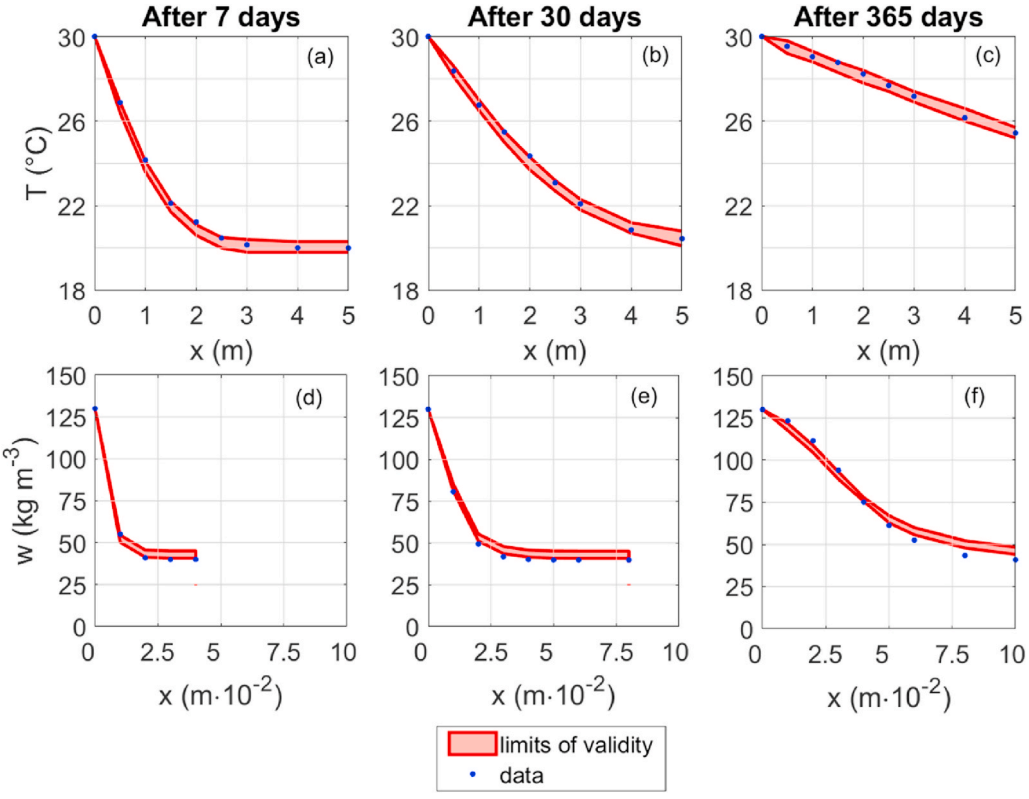

Fig. 3. Temperature (T) and water content (w) distributions along layer thickness (x): data modelled by HMWall (blue dots) and the validity band provided by the EN 15026:2007 (red area). (For interpretation of the references to colour in this figure legend, the reader is referred to the Web version of this article.)

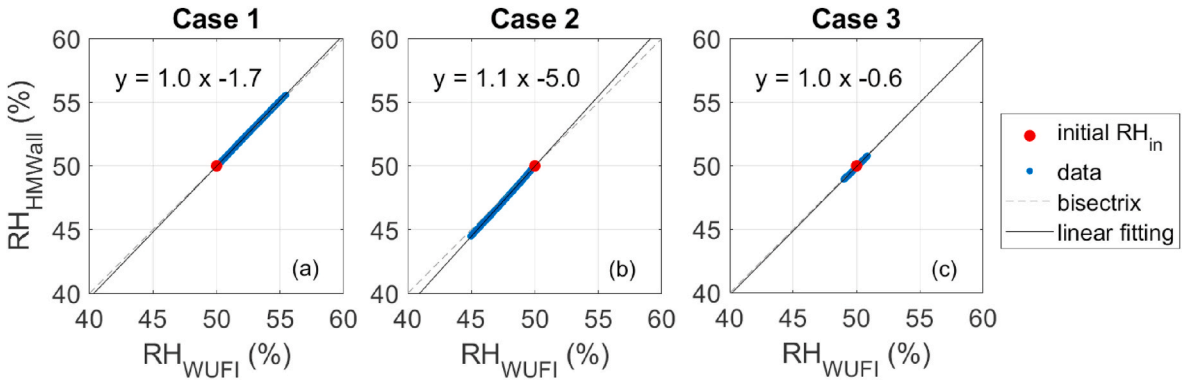

Fig. 4. Scatter diagram of modelled RH values (RH_{HMWall} *versus* RH_{WUFI}) over 8760 h. The indoor initial RH (RH_{in}) is set at 50% (red dot). The linear fitting and its equation are reported. (For interpretation of the references to colour in this figure legend, the reader is referred to the Web version of this article.)

moisture conditions more quickly than WUFI. The difference might be ascribed to the calculation of the liquid transport coefficients for redistribution (D_{ww}): indeed, in HMWall, D_{ww} was always equal to the liquid transport coefficients for suction (D_{ws}), whereas in WUFI, D_{ww} was equal to D_{ws} (equation A.6) except for the water content at RH = 100%, where D_{ww} was set equal to one-tenth of D_{ws}. Refer to Appendix A for a more detailed description of HMWall.

3.1.3. Two parallel rooms with internal moisture and heat gains (exercise 3)

The comparison between the modelled RH values and the experimental measurements is shown in Fig. 5 by means of box-and-whiskers plots for each of the three tests considered (see section 2.3.1).

Left panels of Fig. 5 show a good agreement between modelled and measured RH values in the Reference room in all the tests: the boxes significantly overlapped and the variability of RH values, i.e. the distance between the whiskers, was comparable. RH medians of measurements were 32% (variability of 47%) in Test1, 32% (53%) in Test2 and 48% (49%) in Test3, whereas those of simulations were 32% (variability of 50%), 31% (59%) and 49% (52%), respectively. Concerning the Test room, the building model was able to simulate the RH evolution in accordance with measurements in all tests. Medians were not statistically different (32%, 33% and 46% for measurements and 32%, 33% and 50% for simulation) and the variability differed at most of 5% (60%, 43% and 34% for measurements and 59%, 48% and 36% for simulation). In Test1 of Fig. 5b simulations seem to not perfectly match the RH variability, likely because HMWall was not able to reproduce the poor sorption effect of aluminium foils that coated walls. Conversely, in Test2 (Fig. 5d) and Test3 (Fig. 5f), the sorption effect of gypsum boards on the air RH was well reproduced, although in Test3 the median of modelled

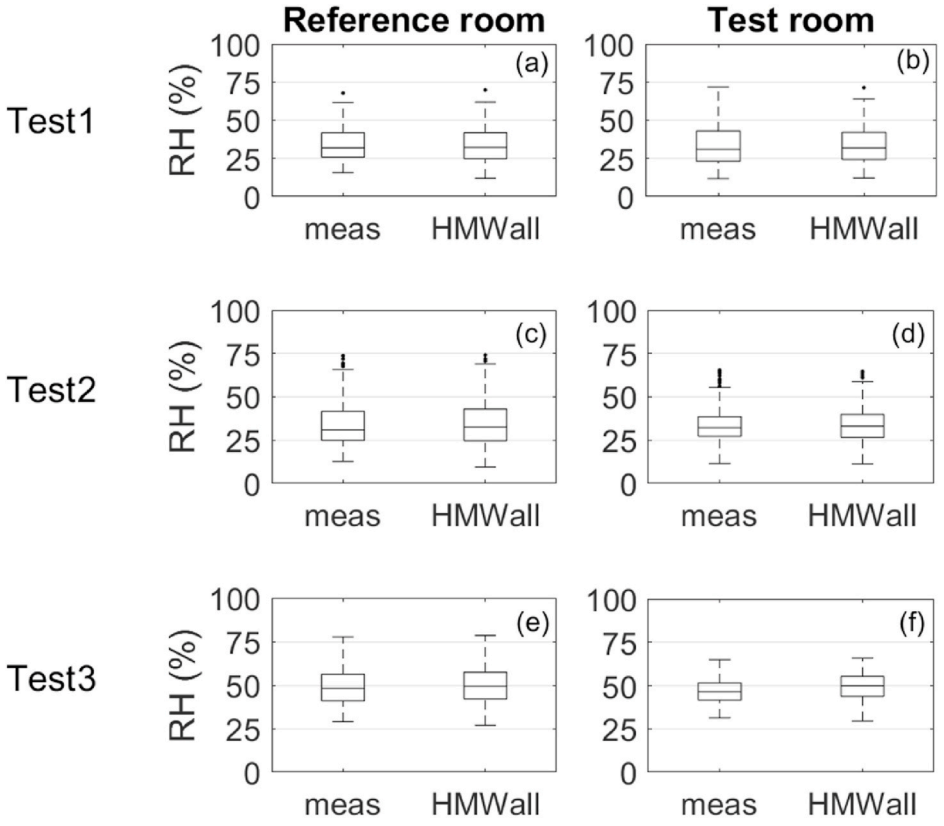

Fig. 5. Box-and-whiskers plots of relative humidity (RH) in Reference room and Test room for test rooms: Test1–aluminium foils on walls; Test2–gypsum boards on walls; Test3–gypsum boards on walls and ceiling.

RH values was slightly higher than the median of measurements.

The Spearman's rank correlation coefficient (rho) was 0.98 in Test1 and 0.96 in Test2, meaning that the building model could reproduce the time evolution of moisture even when moisture peaks and drops occurred. In Test3, rho was slightly lower, although higher than 0.80. In all tests, both MAE and RMSE were found to be less than 4.0%, whereas CV-RMSE was on average 7.6% (never exceeding 11.0%), hence being significantly less than 30%, which is the limit suggested by ASHRAE guideline 14 for hourly calibration [53]. These outcomes make it possible to consider the building model as highly representative of the real site.

As a result, the hygrothermal tool was thoroughly evaluated, encouraging its application also in complex settings.

3.2. Performance assessment of BES + HAM in the historical church

To assess the accuracy of building model B (BES + HAM) with respect to building model A (BES+1D heat transfer), simulations were compared against measurements considering the whole monitoring period from January 1st till March 31st, 2015, as validation outcomes confirmed those of calibration.

QQ plots of modelled *versus* measured values of indoor air T and RH are shown in Fig. 6. The agreement between modelled and measured temperature (Fig. 6a,d) was high for building models. In building model B, all T values within the green band corresponding to ±1 °C were closer to the bisector than those of building model A, meaning that data were equally distributed. MAE and RMSE decreased from 0.3 to 0.4 °C (building model A) to 0.2 °C (building model B), whereas rho was equal to 0.95 (Table 4). The CV-RMSE slightly decreased from building model A (3.0%) to building model B (1.8%), indicating a less residual variance of modelled T values by including the moisture transfer with respect to measurements.

The agreement of modelled RH values with respect to measurements widely changed from building model A to building model B (Fig. 6b,e). If the modelling of walls did not consider the moisture transfer (Fig. 6b), the distribution of modelled RH data highly underestimated the measurements in the range of RH_{meas} between 35 and 60%. Conversely, if the modelling of walls included the simultaneous heat and moisture transfer (e), the agreement between modelled and measured RH values was high in 71% of time (green band, RH = ±5%) and good in 95% of time (dotted band, RH = ±10%). The agreement between modelled and measured data decreased from high to good at the beginning of the simulation (RH_{meas}<30%), as shown in Fig. 7. The enhanced accordance obtained with HMWall was also evident by comparing the statistical metrics: MAE, RMSE and CV-RMSE resulted to be halved with respect to the building model A and rho was equally higher than 0.90 (Table 4).

Table 4
Comparison between building model A (BES+1D heat transfer) and building model B (BES + HAM) in the simulation of the hygrothermal condition inside the church (MAE = mean absolute error; RMSE = root mean square error; CV-RMSE = coefficient of variation of RMSE; rho = Spearman's rank correlation coefficient).

Statistical parameter	Building model A			Building model B		
	T	RH	MR	T	RH	MR
MAE	0.3 °C	8.0%	0.7 $g \cdot kg^{-1}$	0.2 °C	3.6%	0.3 $g \cdot kg^{-1}$
RMSE	0.4 °C	9.3%	0.8 $g \cdot kg^{-1}$	0.2 °C	4.7%	0.4 $g \cdot kg^{-1}$
CV-RMSE (%)	3.0	15.4	14.4	1.8	8.0	8.1
rho	0.95	0.90	0.91	0.95	0.90	0.89

Finally, the agreement between modelled and measured MR values was evaluated (Fig. 6c,f). MR values were always within the band of good agreement (white-dotted band) with both building models, but a better agreement was found with building model B (MR values were within green band more than 95% of time).

In Fig. 7, the time evolution of T (a), RH (b) and MR (c) measurements inside and outside the church is plotted together with the T, RH and MR values modelled by both building models. Indoor T values were smoothed out and less fluctuating than outdoor ones as the result of the high inertia of the building envelope (Fig. 7a). T values modelled by building model A (Fig. 7a, red line) slightly overestimated

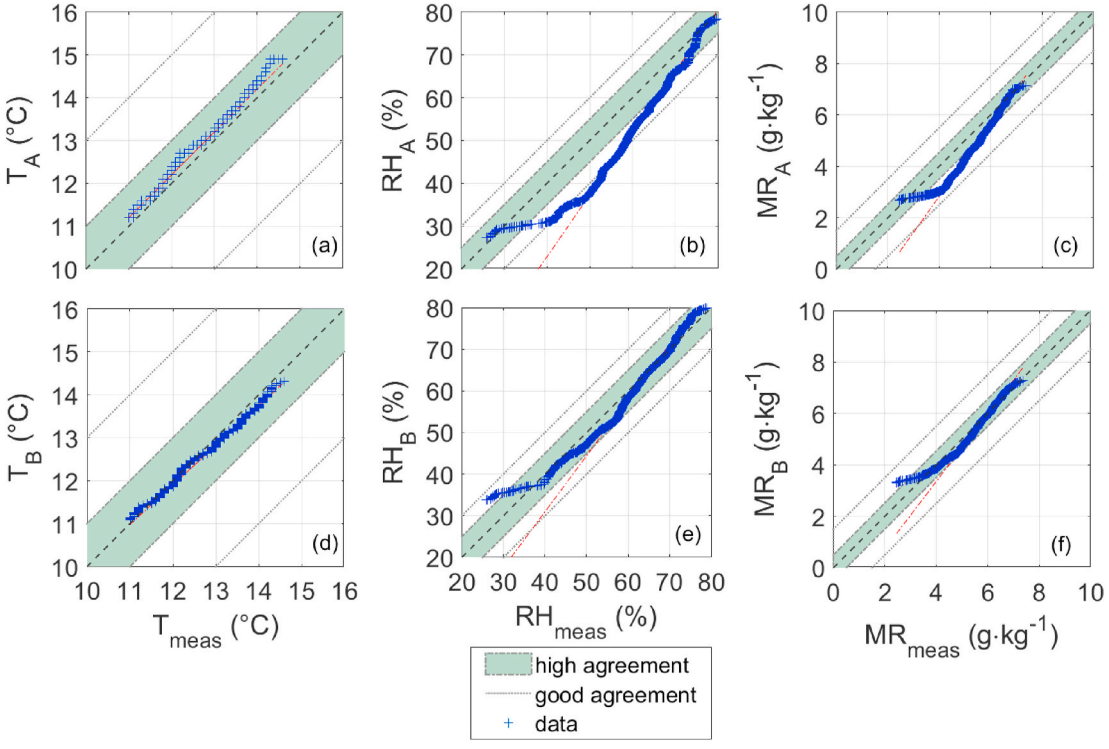

Fig. 6. QQ-plots for temperature (T), relative humidity (RH) and mixing ratio (MR) simulated by building model A (a,b,c) and building model B (d,e,f).

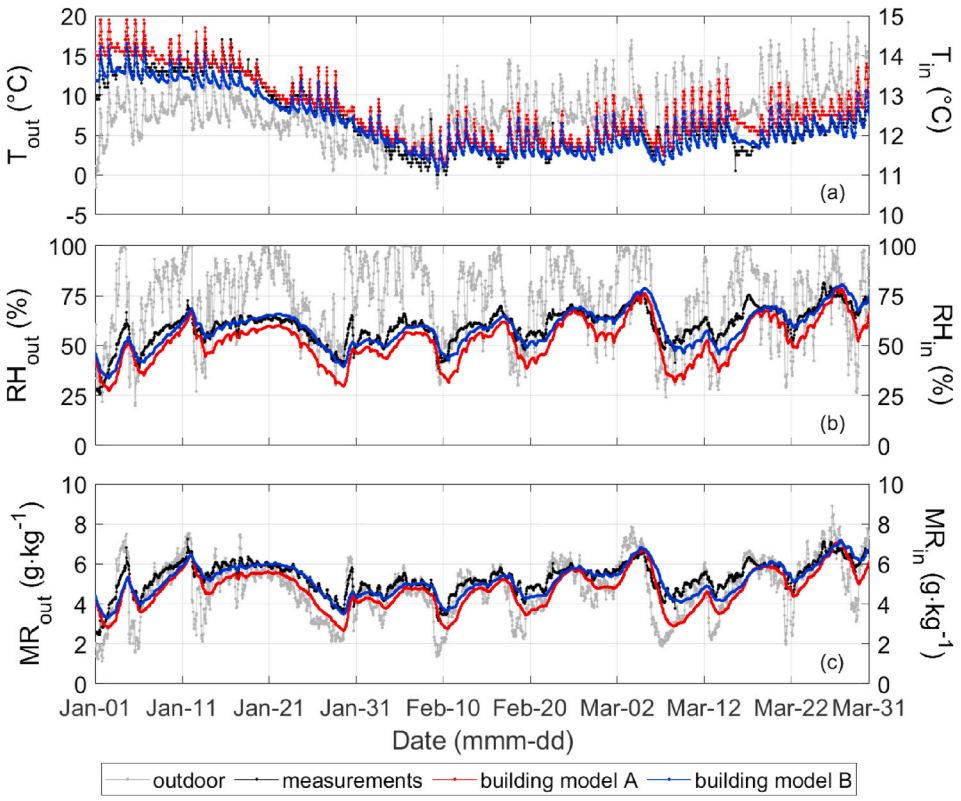

Fig. 7. Time evolution of (a) Temperature, (b) Relative Humidity and (c) Mixing Ratio: indoor and outdoor measurements (black and grey lines), building model A (red line) and building model B (blue line). (For interpretation of the references to colour in this figure legend, the reader is referred to the Web version of this article.)

measurements (Fig. 7a, black line) at the beginning of the simulation and between March 15th-18th, 2015, while T values modelled by building model B (Fig. 7a, blue line) were highly similar to the measurements over the entire simulation. Although the outdoor RH values (Fig. 7b, grey line) strongly influenced the indoor ones (Fig. 7b, black line), it is visible the moisture buffering effect due to the building envelope. As already pointed out, RH values modelled by the two building models were highly correlated with the measurements. However, building model B (Fig. 7b, blue line) simulated the measured RH drops better than building model A (Fig. 7b, red line), because it was able to better reproduce the combined effect of the infiltrations of outdoor air masses and the moisture exchanges between wall surfaces and indoor air masses. This behaviour was also confirmed in MR plot (Fig. 7c), where it is clear that building model B was better able to simulate moisture-mass flows than building model A.

The prediction rate (Qv) for building model A and B was within the ranges in Ref. [12] most of the time, although the results of building model A were slightly better than building model B for $\Delta RH \leq 5\% \cdot day^{-1}$ and $10\% \cdot day^{-1} < \Delta RH \leq 15\% \cdot day^{-1}$ (Table 5). The low rate of compliance of the two building models at $\Delta RH > 15\% \cdot day^{-1}$ was interpreted as related to the moisture internal gains that were not included in the simulations because unknown.

The results showed that the behaviour of RH values inside the church was affected by the combined effect of the air infiltrations, that modulated the relative humidity trend, and the moisture exchanges between air and walls, that governed the short-term variability (RH peaks and drops). Building model B, being able to encompass all the essential features to simulate indoor climate, can be used to investigate preventive conservation measures in the historic church.

Table 5
Evaluation of the prediction rate (Qv) *versus* ΔRH ($\%\cdot day^{-1}$).

ΔRH ($\%\cdot day^{-1}$)	Qv	
	building model A	building model B
≤5	1.00	1.43
>5 and ≤ 10	1.24	0.80
>10 and ≤ 15	0.63	0.06
>15	0.00	0.00
Rate of compliance	high: 0.95≤ Qv ≤ 1.10 good: 0.75≤ Qv < 0.95 and 1.10<Qv ≤ 1.50 low: 0<Qv < 0.75; 1.50<Qv	

3.3. *Diagnostics and conservation in the historical church*

In this step, the hygrothermal simulations of building model A (BES + 1D heat transfer) were compared with those of building model B (BES + HAM) over a calendar year. The aim was to outline an indoor climate scenario that allowed to evaluate the seasonal effect of the outdoor conditions on the indoor ones and to identify potentially risky conditions using both building models A and B.

Fig. 8 shows the seasonal trends of T and MR values modelled inside the church and calculated as monthly averages.

Although the two building models used the same input parameters and boundary conditions, the results in Fig. 8 showed different indoor climate conditions. This difference was due to the integration of the HAM transfer through walls. Both modelled conditions were the indoor climate scenarios inside the church. However, as building model B outperformed building model A both in the calibration and validation periods (section 3.2), it was reasonable to assume that its associated scenario may have more realistically represented the actual indoor climate in the remaining period.

Looking at T plots (Fig. 8a–b), a pattern typical of heavy-masonry buildings is visible: winter and spring values, on average, were above the bisector and summer and autumn values were above the bisector or

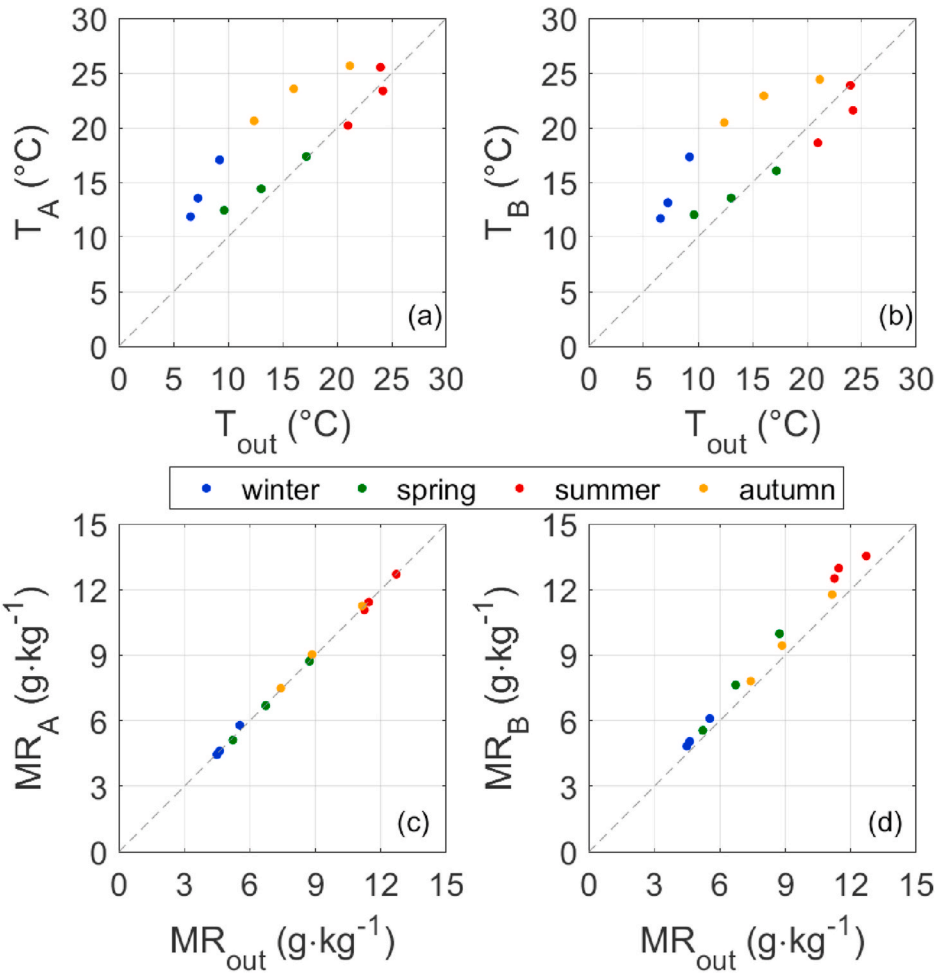

Fig. 8. Outdoor and indoor monthly averages of modelled air temperatures (T) and mixing ratio values (MR) in building model A and building model B.

lie on it. The distribution of T values formed an ellipse as a result of the high thermal inertia of the envelope. Moreover, as the heat flow through walls was computed taking into account the moisture flow (influencing the heat loss), in summer T_B values tended to be lower than T_A.

Looking at MR plots (Fig. 8c-d), data were distributed along the bisector, clearly showing the dependence of the modelled hygric conditions on outdoors. MR_B values (Fig. 8d) were up to 2 $g \cdot kg^{-1}$ higher than the outdoor ones, especially in summer. This behaviour could have been caused by walls releasing moisture or by moisture accumulation due to the poor sorption features of the marble coatings or by the

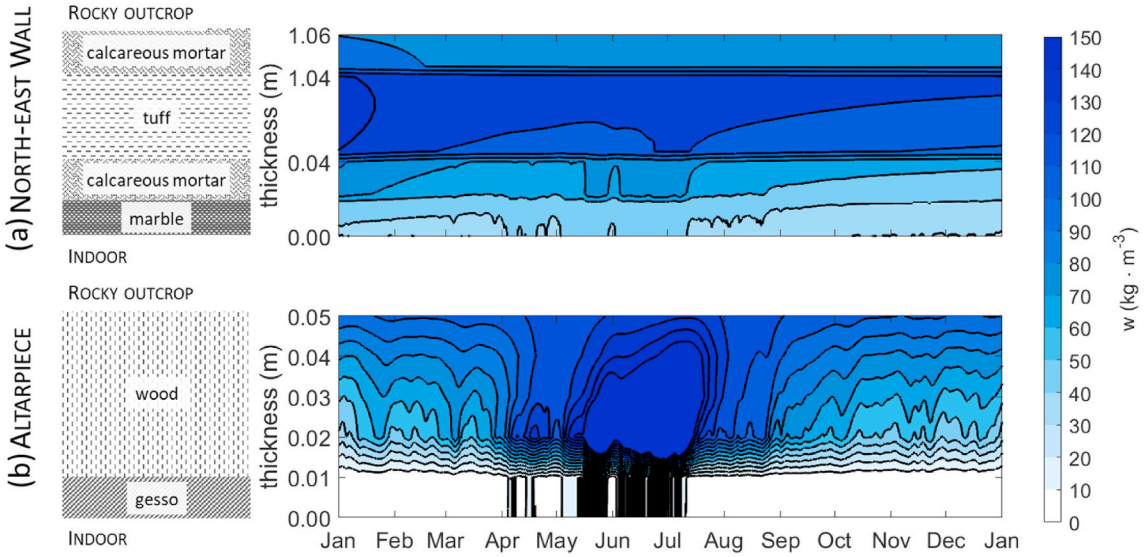

Fig. 9. Water content distribution (w) inside (a) the wall (not equally spaced) and (b) the altarpiece from internal (0.00 m) to external side (rocky outcrop).

combination of the above-mentioned mechanisms.

The north-east wall of the church could be threatened by the damp conditions due to water infiltrations from the rocky outcrop. The back side of the north-east wall and altarpiece (detailed stratigraphy of the partitions are reported in Table 1 and shown in Fig. 9) were set to a constant RH = 95% and RH = 80%, respectively; whereas the front sides were connected to indoor climate conditions of the church. For this reason, the distribution of water content (w) inside the northern wall and the altarpiece was simulated as shown in upper and lower panels of Fig. 9, respectively. This analysis allowed to diagnose the formation of a moisture gradient within the wall components, thus providing a better evaluation of the potential moisture-induced degradation.

Fig. 9a clearly shows that one year of simulation could not be representative of the moisture content (w) distribution inside the wall since different conditions in the middle of the stratigraphy are visible at the beginning and at the end of simulation. This behaviour is typical of ancient thick masonries, in which moisture flows are slower than those in thinner partitions. As expected, the thin stratigraphy of the panel paintings (Fig. 9b) did not show the same behaviour.

Moreover, this analysis demonstrated that two months of initialisation were not enough to capture the slow moisture transfer in thick masonries. In addition, if only one year of simulation is considered, the moisture content distribution across the wall can be also affected by the initial values set in the simulation.

The most critical period was found to be between April and July, when a higher w gradient occurred in both partitions. In the case of the masonry, a w gradient of 60 $kg \cdot m^{-3}$ could trigger crystallisation/dissolution cycles of soluble salts, causing the risk of mechanical degradation of the wall coatings (e.g. detachments of marble layers). In addition, higher w values occurring in the inner layers could favour interstitial condensation, detrimental for the conservation of walls. In the case of the altarpiece, simulated w values were stable between 0 $kg \cdot m^{-3}$ and 10 $kg \cdot m^{-3}$ in the first 0.01 m, whereas a gradient of 40 $kg \cdot m^{-3}$ occurred between 0.01 and 0.02 m and up to 150 $kg \cdot m^{-3}$ in summer due to higher indoor MR values (Fig. 8d).

The behaviour described above could be responsible for stresses to moisture-sensitive and multi-layered artworks, such as the altarpiece, jeopardizing their conservation.

4. Conclusions

The hygrothermal modelling of historical churches is a promising approach to study preservation issues and appropriate strategies for mitigating climate-induced conservation risks. In this context, difficulties can arise in the use of Heat, Air and Moisture (HAM) models into building energy simulation (BES) and the performance of the hygrothermal tool has to be properly assessed to accurately model indoor climate conditions.

This research aimed to investigate the capabilities of BES extended with a HAM model (HMWall) for diagnostics and conservation of historical buildings. To this purpose, a multi-step methodology was conceived and used to assess the performance of the simulation tool from standardised exercises to a complex site. The methodology was thus applied to the historical church of the 17th-century *Chiesa di Santa Rosalia* (Italy), allowing to explore climate-induced conservation risks based on simulations.

The first step of the methodology allowed to exclude incorrect assumptions and calculations in HMWall encompassing the criteria defined in ANSI ASHRAE Standard 140 (section 3.1). This result was preparatory to the hygrothermal modelling of the historical site. The second step compared indoor climate simulations from the hygrothermal modelling of *Chiesa di Santa Rosalia* using BES with either a 1D heat transfer only (building model A) or a HAM transfer (building model B). Building model B improved the simulation accuracy by +50% with respect to building model A. Moreover, building model B proved to be able to reproduce the indoor moisture balance depending simultaneously on infiltrations and on vapour mass flow exchanges with the walls, otherwise left out by the 1D heat transfer model (section 3.2). Finally, annual simulations allowed to compare the indoor climate scenarios resulting from the hygrothermal modelling with and without the HAM transfer (section 3.3). The analysis also explored the capability of hygrothermal modelling with HAM transfer to describe deterioration. For example, the distribution of moisture content in partitions affected by water infiltrations was studied as potentially responsible for mechanical stresses to moisture-sensitive and multi-layered artworks.

This study highlighted some relevant aspects of the hygrothermal modelling of the indoor climate conditions in historical churches. First, standardised exercises are useful to objectively evaluate the performance of BES + HAM tools. Second, hygrothermal models with HAM give the chance to study moisture-induced deterioration risks through the simulation of the moisture content distribution in partitions. Furthermore, this analysis put in evidence the importance of the initialisation period, which should be long enough to cover the period representing the slow moisture flow in thick masonries. A penalty of our work was that the calibration was carried out only in winter; therefore, the hygrothermal simulation over the period without measurements might be not fully representative of the actual indoor climate inside the church. If a calendar year of measurements had been available, the building model would have been more accurate becoming a more robust tool for the simulation of indoor climate inside the church.

Although this study does not exhaust the topic, the conceived methodology could be exploited also for the performance assessment of other hygrothermal simulation tools in other application fields.

Declaration of competing interest

The authors declare that they have no known competing financial interests or personal relationships that could have appeared to influence the work reported in this paper.

Acknowledgement

Frasca F. thanks Dr Florian Antretter (Hygrothermics Department of Fraunhofer Institute for Building Physics - IBP) for his technical advices during her visiting period in the IBP in 2017. Authors are thankful to Principe Don Benedetto Barberini for giving consent for the case study to be used in this research, Arch. Nicoletta Marconi for the historical support and Serena Contardi for the acquisition of indoor climate data. Finally, authors are grateful to Tecno.El S.r.l. for the indoor climate monitoring system. The authors also thank the anonymous reviewers for the valuable comments to improve the manuscript. Frasca F., Siani A.M. and Verticchio E. thank for the financial support of the APC the CollectionCare project (European Union's Horizon 2020 research and innovation programme under grant agreement No 814624).

Appendix A. The HMWall model: a HAM model in IDA ICE

IDA Indoor Climate and Energy (IDA ICE 4.7.1) software, distributed by EQUA simulation AB, can be extended with HMWall, which simulates the 1D heat and moisture transfer through walls. HMWall can be used in IDA ICE either as a single independent wall-object or as a wall-component of a larger building system [44,54].

The moisture storage curve (equation A.1) is calculated as a function of relative humidity as follows:

$$w(\phi) = w_f \times \frac{(\beta - 1) \times \phi}{\beta - \phi} \tag{A.1}$$

where w is the water content ($kg \cdot m^{-3}$), w_f is the free water saturation ($kg \cdot m^{-3}$), ϕ is the relative humidity (−) and β is the approximation factor (−) [55].

The simultaneous heat (equation A.2) and moisture (equation A.3) transport equations are:

$$\frac{dH}{dT} \times \frac{\partial T}{\partial t} = \nabla(\lambda \times \nabla T) - h_v \times \nabla g_v \tag{A.2}$$

$$\frac{dw}{d\phi} \times \frac{\partial \phi}{\partial t} = \nabla(\nabla g_v + \nabla g_w) \tag{A.3}$$

where dH/dT is the heat storage capacity of the moist material ($J \cdot m^{-3} \cdot K^{-1}$); $\partial T/\partial t$ is the rate of temperature (T) ($K \cdot s^{-1}$); λ is the thermal conductivity of the wet material ($W \cdot m^{-1} \cdot K^{-1}$) (equation A.4); $h_v \times \nabla g_v$ is the latent heat source where h_v is the evaporation enthalpy of water ($J \cdot kg^{-1}$) and ∇g_v is the vapour diffusion flux ($kg \cdot m^{-2} \cdot s^{-1}$). In eq. A.3, dw/dϕ is the moisture storage capacity ($kg \cdot m^{-3}$); $\partial\phi/\partial t$ is the rate of relative humidity (−); ∇g_w is the capillary moisture flux ($kg \cdot m^{-2} \cdot s^{-1}$) and is expressed as $D_\phi \times \nabla\phi$ with D_ϕ as the liquid conduction coefficient of water ($kg \cdot m^{-1} \cdot s^{-1}$) (equation A.5); ∇g_v is the vapour diffusion flux ($kg \cdot m^{-2} \cdot s^{-1}$) and is expressed as $(\delta_a/\mu) \times \nabla(\phi \times p_{sat})$ with δ_a the water vapour permeability of air [56], μ the dimensionless vapour resistance factor of material and p_{sat} as the saturated vapour pressure (Pa). The model considers μ as a constant value in the RH range.

$$\lambda(w) = \lambda_d \times \frac{1 + b \times w}{\rho} \tag{A.4}$$

where λ_d is the dry thermal conductivity ($W \cdot m^{-1} \cdot K^{-1}$); b the thermal conductivity supplement and ρ the material density ($kg \cdot m^{-3}$).

The liquid conduction coefficient (D_ϕ) is calculated assuming no difference between suction and redistribution [55].

$$D_\phi = D_{ws} \times \frac{dw}{d\phi} \tag{A.5}$$

where D_{ws} -liquid transport coefficient for suction- is calculated as equation A.6:

$$D_{ws} = 3.8 \times \left(\frac{A_w}{w_f}\right)^2 \times 1000^{\frac{w}{w_f}-1} \tag{A.6}$$

where A_w is the water penetration coefficient and w_f is the free water saturation ($kg \cdot m^{-3}$).

Funding sources

The APC was funded by CollectionCare project, which has received funding from the European Union's Horizon 2020 research and innovation programme under grant agreement No 814624.

Authors' contribution

All the authors have equally contributed to this study.

References

[1] Vincoli in rete. http://vincoliinrete.beniculturali.it/VincoliInRete/vir/statistics/redirectReport3. (Accessed 31 July 2020).

[2] A. Mleczkowska, M. Strojecki, Ł. Bratasz, R. Kozłowski, Particle penetration and deposition inside historical churches, Build. Environ. 95 (2016) 291–298, https://doi.org/10.1016/j.buildenv.2015.09.017.

[3] F. Frasca, E. Verticchio, A. Caratelli, C. Bertolin, D. Camuffo, A.M. Siani, A comprehensive study of the microclimate-induced conservation risks in hypogeal sites: the Mithraeum of the baths of caracalla (Rome), Sensors 20 (11) (2020) 3310, https://doi.org/10.3390/s20113310.

[4] M.J. Varas-Muriel, R. Fort, M.I. Martínez-Garrido, A. Zornoza-Indart, P. López-Arce, Fluctuations in the indoor environment in Spanish rural churches and their effects on heritage conservation: hygro-thermal and CO2 conditions monitoring, Build. Environ. 82 (2014) 97–109, https://doi.org/10.1016/j.buildenv.2014.08.010.

[5] T. Kalamees, A. Väli, L. Kurik, M. Napp, E. Arümagi, U. Kallavus, The influence of indoor climate control on risk for damages in naturally ventilated historic churches in cold climate, Int. J. Architect. Herit. 10 (4) (2016) 486–498, https://doi.org/10.1080/15583058.2014.1003623.

[6] F. Frasca, A.M. Siani, G.R. Casale, M. Pedone, M. Strojecki, A. Mleczkowska, Assessment of indoor climate of Mogiła Abbey in Kraków (Poland) and the application of the analogues method to predict microclimate indoor conditions, Environ. Sci. Pollut. Control Ser. 24 (16) (2017) 13895–13907, https://doi.org/10.1007/s11356-016-6504-9.

[7] D. Camuffo, E. Pagan, S. Rissanen, Ł. Bratasz, R. Kozłowski, M. Camuffo, A. della Valle, An advanced church heating system favourable to artworks: a contribution to European standardisation, J. Cult. Herit. 11 (2) (2010) 205–219, https://doi.org/10.1016/j.culher.2009.02.008.

[8] EN 15759-1, Conservation of Cultural Property - Indoor Climate - Part 1: Guidelines for Heating Churches, Chapels and Other Places of Worship, European Committee for Standardization (CEN), Brussels, 2011.

[9] E. Verticchio, F. Frasca, F.J. Garcìa-Diego, A.M. Siani, Investigation on the use of passive microclimate frames in view of the climate change scenario, Climate 7 (8) (2019) 98, https://doi.org/10.3390/cli7080098.

[10] J. Leissner, R. Kilian, L. Kotova, D. Jacob, U. Mikolajewicz, T. Broström, J. Ashley-Smith, H.L. Schellen, M. Martens, J. van Schijndel, F. Antretter, M. Winkler, C. Bertolin, D. Camuffo, G. Simeunovic, T. Vyhlídal, Climate for Culture: assessing the impact of climate change on the future indoor climate in historic buildings using simulations, Heritage Science 3 (1) (2015) 1–15, https://doi.org/10.1186/s40494-015-0067-9.

[11] H.L. Schellen, A.W.M. Van Schijndel, Setpoint control for air heating in a church to minimize moisture related mechanical stress in wooden interior parts, Building Simulation 4 (1) (2011, March) 79–86, https://doi.org/10.1007/s12273-011-0026-7.

[12] V. Rajčić, A. Skender, D. Damjanović, An innovative methodology of assessing the climate change impact on cultural heritage, Int. J. Architect. Herit. 12 (1) (2018) 21–35, https://doi.org/10.1080/15583058.2017.1354094.

[13] G.B. Coelho, H.E. Silva, F.M. Henriques, Calibrated hygrothermal simulation models for historical buildings, Build. Environ. 142 (2018) 439–450, https://doi.org/10.1016/j.buildenv.2018.06.034.
[14] A. Sadłowska-Sałęga, J. Radoń, Feasibility and limitation of calculative determination of hygrothermal conditions in historical buildings: case study of st. Martin church in Wiśniowa, Build. Environ. 186 (2020) 107361, https://doi.org/10.1016/j.buildenv.2020.107361.
[15] C.M. Muñoz-González, A.L. León-Rodríguez, J. Navarro-Casas, Air conditioning and passive environmental techniques in historic churches in Mediterranean climate. A proposed method to assess damage risk and thermal comfort pre-intervention, simulation-based, Energy Build. 130 (2016) 567–577, https://doi.org/10.1016/j.enbuild.2016.08.078.
[16] C.M. Muñoz-González, A.L. León-Rodríguez, M. Campano-Laborda, C. Teeling, R. Baglioni, The assessment of environmental conditioning techniques and their energy performance in historic churches located in Mediterranean climate, J. Cult. Herit. 34 (2018) 74–82, https://doi.org/10.1016/j.culher.2018.02.012.
[17] M. Napp, M. Wessberg, T. Kalamees, T. Broström, Adaptive ventilation for climate control in a medieval church in cold climate, Int. J. Vent. 15 (1) (2016) 1–14, https://doi.org/10.1080/14733315.2016.1173289.
[18] M. Napp, T. Kalamees, Energy use and indoor climate of conservation heating, dehumidification and adaptive ventilation for the climate control of a mediaeval church in a cold climate, Energy Build. 108 (2015) 61–71, https://doi.org/10.1016/j.enbuild.2015.08.013.
[19] G. Semprini, C. Galli, S. Farina, Reuse of an ancient church: thermal aspect for integrated solutions, Energy Procedia 133 (2017) 327–335, https://doi.org/10.1016/j.egypro.2017.09.395.
[20] A. Hayati, M. Mattsson, M. Sandberg, Single-sided ventilation through external doors: measurements and model evaluation in five historical churches, Energy Build. 141 (2017) 114–124, https://doi.org/10.1016/j.enbuild.2017.02.034.
[21] A. Hayati, Measurements and modeling of airing through porches of a historical church, Sci. Technol.Built. Environ. 24 (3) (2018) 270–280, https://doi.org/10.1080/23744731.2017.1388132.
[22] Muñoz-González, C.M.M. González, A.L. Rodríguez, R.S. Medina, J.R. Jaramillo, Effects of future climate change on the preservation of artworks, thermal comfort and energy consumption in historic buildings, Appl. Energy 276 (2020) 115483, https://doi.org/10.1016/j.apenergy.2020.115483.
[23] D. Camuffo, Microclimate for Cultural Heritage 3rd Edition Measurement, Risk Assessment, Conservation, Restoration, and Maintenance of Indoor and Outdoor Monuments, Elsevier, Amsterdam, 2014.
[24] G.G. Akkurt, N. Aste, J. Borderon, A. Buda, M. Calzolari, D. Chung, F. Leonforte, Dynamic thermal and hygrometric simulation of historical buildings: critical factors and possible solutions, Renew. Sustain. Energy Rev. 118 (2020) 109509, https://doi.org/10.1016/j.rser.2019.109509.
[25] M. Barclay, N. Holcroft, A.D. Shea, Methods to determine whole building hygrothermal performance of hemp–lime buildings, Build. Environ. 80 (2014) 204–212, https://doi.org/10.1016/j.buildenv.2014.06.003.
[26] T. Colinart, P. Glouannec, Temperature dependence of sorption isotherm of hygroscopic building materials. Part 1: experimental evidence and modeling, Energy Build. 139 (2017) 360–370, https://doi.org/10.1016/j.enbuild.2016.12.082.
[27] M. Andreotti, D. Bottino-Leone, M. Calzolari, P. Davoli, L. Dias Pereira, E. Lucchi, A. Troi, Applied research of the hygrothermal behaviour of an internally insulated historic wall without vapour barrier: in situ measurements and dynamic simulations, Energies 13 (13) (2020) 3362, https://doi.org/10.3390/en13133362.
[28] A. Holm, H.M. Kuenzel, K. Sedlbauer, The hygrothermal behaviour of rooms: combining thermal building simulation and hygrothermal envelope calculation, in: Eighth International IBPSA Conference, vol. 1, 2003, August, pp. 499–505 (Eindhoven Netherlands).
[29] H.L. Hens, Combined heat, air, moisture modelling: a look back, how, of help? Build. Environ. 91 (2015) 138–151, https://doi.org/10.1016/j.buildenv.2015.03.009.
[30] C. Gomes, C. Thule, D. Broman, P.G. Larsen, H. Vangheluwe, Co-simulation: a survey, ACM Computing Surveys (CSUR) 51 (3) (2018) 1–33, https://doi.org/10.1145/3179993.
[31] M. Steeman, M. De Paepe, A. Janssens, Impact of whole-building hygrothermal modelling on the assessment of indoor climate in a library building, Build. Environ. 45 (7) (2010) 1641–1652, https://doi.org/10.1016/j.buildenv.2010.01.012.
[32] L. Havinga, H. Schellen, Applying internal insulation in post-war prefab housing: understanding and mitigating the hygrothermal risks, Build. Environ. 144 (2018) 631–647, https://doi.org/10.1016/j.buildenv.2018.08.035.
[33] M.Y. Ferroukhi, R. Djedjig, K. Limam, R. Belarbi, Hygrothermal behavior modeling of the hygroscopic envelopes of buildings: a dynamic co-simulation approach, In Building Simulation 9 (5) (2016, October) 501–512, https://doi.org/10.1007/s12273-016-0292-5. Tsinghua University Press.
[34] M. Napp, T. Kalamees, T. Tark, E. Arumägi, Integrated design of Museum's indoor climate in medieval episcopal castle of haapsalu, Energy Procedia 96 (2016) 592–600, https://doi.org/10.1016/j.egypro.2016.09.105.
[35] F. Frasca, C. Cornaro, A.M. Siani, A method based on environmental monitoring and building dynamic simulation to assess indoor climate control strategies in the preventive conservation within historical buildings, Sci. Technol.Built. Environ. 25 (9) (2019) 1253–1268, https://doi.org/10.1080/23744731.2019.1642093.
[36] T. Busser, M. Pailha, A. Piot, M. Woloszyn, Simultaneous hygrothermal performance assessment of an air volume and surrounding highly hygroscopic walls, Build. Environ. 148 (2019) 677–688, https://doi.org/10.1016/j.buildenv.2018.11.031.
[37] J. Straube, E.F.P. Burnett, Overview of hygrothermal (HAM) analysis methods, in: H.R. Trechsel (Ed.), ASTM Manual 40 - Moisture Analysis and Condensation Control in Building Envelopes, 1991, pp. 81–89 [chapter 5].
[38] EN 15758, Conservation of Cultural Property - Procedures and Instruments for Measuring Temperatures of the Air and the Surfaces of Objects, European Committee for Standardization (CEN), Brussels, 2010.
[39] EN 16242, Conservation of Cultural Heritage - Procedures and Instruments for Measuring Humidity in the Air and Moisture Exchanges between Air and Cultural Property, European Committee for Standardization (CEN), Brussels, 2012.
[40] N. Marconi, E. Eramo, La chiesa di Santa Rosalia nel palazzo dei principi Barberini a Palestrina: committenza e cantiere,» Studi e Ricerche di Storia dell'Architettura, Rivista dell'Associazione Italiana Storici dell'Architettura (2017) 46–65.
[41] EN ISO 13370, Thermal Performance of Buildings – Heat Transfer via the Ground – Calculation Methods, European Committee for Standardization (CEN), Brussels, 2017.
[42] MASEA certified database, Available: https://www.masea-ensan.de/. (Accessed 25 June 2020).
[43] A.A. Hegazy, Effect of dust accumulation on solar transmittance through glass covers of plate-type collectors, Renew. Energy 22 (4) (2001) 525–540, https://doi.org/10.1016/S0960-1481(00)00093-8.
[44] EN 15026, Hygrothermal Performance of Building Components and Building Elements - Assessment of Moisture Transfer by Numerical Simulation, International Organization for Standardization, Geneva, 2007.
[45] F. Frasca, C. Cornaro, A.M. Siani, Performance assessment of a heat and moisture dynamic simulation model in IDA ICE by the comparison with WUFI Plus, IOP Conf. Ser. Mater. Sci. Eng. 364 (2018), 012024, https://doi.org/10.1088/1757-899X/364/1/012024.
[46] M. Woloszyn, C. Rode, Tools for performance simulation of heat, air and moisture conditions of whole buildings, Building Simulation 1 (1) (2008) 5–24, https://doi.org/10.1007/s12273-008-8106-z.
[47] R. Judkoff, J. Neymark, Model validation and testing: the methodological foundation of ASHRAE Standard 140, Build. Eng. 112 (2) (2006) 367–376.
[48] A.A. Hamid, P. Wallentén, Hygrothermal assessment of internally added thermal insulation on external brick walls in Swedish multifamily buildings, Build. Environ. 123 (2017) 351–362, https://doi.org/10.1016/j.buildenv.2017.05.019.
[49] Z. Pasztory, P.N. Peralta, S. Molnar, I. Peszlen, Modeling the hygrothermal performance of selected North American and comparable European wood-frame house walls, Energy Build. 49 (2012) 142–147, https://doi.org/10.1016/j.enbuild.2012.02.003.
[50] J. Maia, N.M. Ramos, R. Veiga, Evaluation of the hygrothermal properties of thermal rendering systems, Build. Environ. 144 (2018) 437–449, https://doi.org/10.1016/j.buildenv.2018.08.055.
[51] Climate for culture. WP 3. Hygrothermal building simulation, Available: https://www.climateforculture.eu/index.php?inhalt=project.workpackages. (Accessed 10 December 2020).
[52] H.E. Huerto-Cardenas, F. Leonforte, N. Aste, C. Del Pero, G. Evola, V. Costanzo, E. Lucchi, Validation of Dynamic Hygrothermal Simulation Models for Historical Buildings: State of the Art, Research Challenges and Recommendations, Building and Environment, 2020, https://doi.org/10.1016/j.buildenv.2020.107081, 107081.
[53] ASHRAE Guideline 14, Measurement of Energy and Demand Savings, American Society of Heating and Air-Conditioning Engineers, Inc., Atlanta, 2002.
[54] J. Kurnitski, M. Vuolle, Simultaneous Calculation of Heat, Moisture, and Air Transport in a Modular Simulation Environment, Estonian Academy Publishers, 2000, pp. 25–47.
[55] H.M. Künzel, Simultaneous Heat and Moisture Transport in Building Components. One-And Two-Dimensional Calculation Using Simple Parameters, IRB-Verlag, Stuttgart, 1995.
[56] P. Slanina, Š. Šilarová, Moisture transport through perforated vapour retarders, Build. Environ. 44 (8) (2009) 1617–1626, https://doi.org/10.1016/j.buildenv.2008.10.006.